Rule-based Learning Techniques to Derive Automated Digital Terrain Model Using Airborne LiDAR Data

Jifroudi, H. M.,[1,3*] Mansor, S. B.[1] and Pradhan, B.[2]
[1]Geospatial Information Science Research Center (GISRC), Faculty of Engineering, Universiti Putra Malaysia (UPM), 43400 Serdang, Selangor, Malaysia, E-mail: hrmaskani@yahoo.com*
[2]Centre for Advanced Modelling and Geospatial Information Systems (CAMGIS), Faculty of Engineering and IT, University of Technology Sydney, Sydney, NSW, Australia
[3]Environmental Research Institute, Academic Center for Education, Culture and Research (ACECR), Guilan, Iran
**Corresponding Author*

DOI: https://doi.org/10.52939/ijg.v18i6.2459

Abstract
Constructing an accurate Digital Terrain Model is costly and time-consuming, leading to more challenges in urban environments due to the presence of different objects. This research performs the step by step analysis of LiDAR data using a rule-based algorithm to create an automatic DTM. This method needs no extra data and has a precision equal to that of a DTM, which is constructed manually. The DTM constructed in this research was compared to the DTM constructed manually to investigate the accuracy of the results. It was found that the mean difference between the elevations in both DTMs in the rural and urban areas was equal to zero and 0.10 m, respectively, while the mean difference between the slopes was 1.2 and 1.6%, respectively. However, in the areas which lacked buildings, the elevation and slope characteristics were equal, revealing identical DTMs, which was also confirmed by sig=.441 from t-test. Although sig=0.0 in the t-test shows a difference between the two DTMs in the urban and rural areas, it does not reveal the value of this difference. Thus, the RMSE method was used to examine this difference, leading to the values of ±0.20m, ±0.05m, and ±0.04m for the urban, rural, and areas without buildings, respectively. Considering that the precision required for urban and rural planning is 0.4m, it is totally acceptable to use the proposed algorithm instead of the manual method.

Keywords: Digital Terrain Model, Light Detection and Ranging, Rule-based learning, Rural area, Urban area

1. Introduction

The surface shape, shown by the Digital Terrain Model (DTM), displays the earth's surface using points with specific coordinates [1] in the raster format, which is one of the main products of photogrammetry and remote sensing [2] and [3] and the basis for many applied projects [4] [5] and [6]. It has always attracted the attention of many experts because the accuracy of the DTM can dramatically change the research results [7]. However, many research works that use DTM as an information layer, employ commercial software [8], the majority of which use the data without applying necessary filters, although filtering contributes substantially to creating an accurate DTM [9] and [10]. In addition, filtering LiDAR data needs time and specialty, which depends on the experts' experience [11] and [12] and is not always possible for many executive and research projects. The importance of this issue becomes more apparent when carefully reviewing the research by Klapste et al., [13] on DTMs generated by some software. Although the area studied by them did not have man-made structures, and the experts had previously visited the points, the RMSE results showed values in the range of 0.13 to 0.19m. Therefore it is essential to strictly investigate the accuracy of the generated DTMs by the common software in the urban areas, especially where no initial review of the LiDAR points has taken place.

Furthermore, the need for an accurate DTM in studies based on extensive details such as surface water and flood management [14] is an undeniable fact. However, from the theoretical point of view, LiDAR can create a digital elevation model of the earth's surface with high speed and accuracy compared to the traditional methods [15] [16] and [17].

Yet, the extraction of the digital elevation model from urban areas and complex and uneven environments is challenging, even using modern methods [18] [19] and [10]. Hence, the accurate DTM is only obtained when the non-ground points are properly filtered [20] and [21] and correctly interpolated. Despite all studies conducted, building an accurate DTM has always been a serious challenge in applied research [22] and [23]. The methods for accurate generation of DTM are applicable only when the experts can use them like the available commercial software without the need for specific knowledge.

1.1 Literature Review

Perhaps filtering based on a specific window can be used as one of the oldest DTM development methods that have evolved. Kilian et al., [24] and Zhang et al., [25] used this method, indicating that if the correct information on the region is provided, the resulting DTM has adequate accuracy. The slope-based method has been also used to separate the ground and non-ground points. This method initially considers a point as a ground point, which serves as the basis for the measurement of other points [26] and [27]. Sohn and Dowman [28] proposed a method, which first created a network with several initial points, and then a decision was made based on the angle of each point concerning the surrounding points to omit or keep the point as a non-ground or ground point, respectively. To improve this method, the initial points for triangulation were selected from the corners of the region, and the remaining points were classified into the upper and lower groups of initial triangulation. Afterward, the conditions of triangulation angles were studied separately for each group.

In 2009, Meng et al., [20] attempted to compare the properties of each point with the four points around it and created a filter based on four different types. Although this filter had satisfactory results, interpolation based on the independent value of each point, especially in large buildings, was not satisfying due to the drastic height variations on the building boundary.

Baligh Jahromi et al., [29] used an artificial neural network to omit the non-ground points. This method is based on the height difference between the first and last reflections. However, it cannot be used to develop DTM with fast processing due to the multiplicity of the constraints on the angles defined and the need for sample data. On the other hand, steep slopes are a limiting factor in this method, leading to numerous challenges in the practical application of this method in operational programs. In 2016, Zhang et al., [30] conducted a study of DTM extraction from DSM and stated that it is substantially important to separate non-ground points from the ground points for the automatic extraction of DTM from LIDAR data. This study sought to extract DTM from DSM with low resolution, using a two-step filter. The experiments on the resulting DTM showed significant effectiveness of the method for data with spatial resolution of 10 to 30 meters. However, the algorithm can be only used for large areas to provide an overall view and cannot be used for urban areas that call for high accuracy.

Wojciech [31] carried out a study on building DTM using the kriging method and tried to examine the usual interpolation methods to create an accurate DTM. They examined the inverse distance weighing, the nearest neighbor, the moving average, and kriging algorithms. This study aimed to analyze the characteristics of the results of each of the existing interpolation methods to considerably reduce the computation time while maintaining the highest accuracy level in the created model. The experimental results highlighted significant advantages of the kriging technique over the other methods.

1.2 Objective and Research Gap

Generating accurate and applicable DTMs remains a serious but essential challenge [10] [32] [33] and [34]. Although all the previous studies have sought to generate accurate DTMs, due to the complexity of the used filters [10] and [11] in a section of research process, they have taken advantage of one stage of the specialist supervision. This would result in two problems: 1) when the DTM layer generation is not the primary objective, but researchers utilize DTM as one of the necessary layers of information, it is not possible to implement essential modifications through field visits or taking advantage of experienced experts. Thus, they prefer to use raw data and commonly available software. 2) As the factors, which the experts should examine for the generation of DTM, are numerous and related to the human experience, certainly there will be errors during the investigation process. Therefore, the methods presented in the research works are only operative when the proposed algorithm can generate the required DTMs automatically without the need for further data or expert information. In reality, the most authentic method, which is the manual method [17], requires extensive time and costs, making its application impossible in the research and executive projects.

Therefore, an important point to note is that the DTM has applications in a broad spectrum of research works and operational projects. In many projects, DTM is just one of the layers used, which can significantly affect the results. Previous research works have largely ignored the fact that although a complex, time-intensive method can lead to an accurate DTM, this process is not practically feasible for other research works and operational projects as it demands for long processing times and an expert who is familiar with the generation process of DTM. Accordingly, a clear research gap in the existing literature is the failure to pay adequate attention to the practical applicability of the proposed DTM production methods to ensure their usability for all researchers and experts who have no expertise in DTM generation.

Therefore, creating a fully automatic structure is one of the main goals of this research. For this purpose, the LiDAR data are implemented because LiDAR data provide the possibility to transfer geographical location and elevation characteristics and much other information about the land objects in the form of point clouds. On the other hand, it is possible to convert LiDAR data into a multidimensional matrix, which subsequently helps with using the programming languages in the analysis of the above mentioned data. This research has the Python programming language to write a program which initially accepts the LiDAR data file, executes a number of rule-based algorithms, and finally stores the DTM file with the raster format in the exit path.

2. Materials and Methods

2.1 Study Area

The study region with a surface area of 3000ha is located in the west of Malaysia, southeast of Selangor Province. The coordinates of the aforementioned region in the UTM coordinates system in the region N47 are as follows: minimum x = 800000, maximum X = 805000, minimum Y = 328000, and maximum Y = 334000 (Figure 1). The study region is divided into three major parts concerning texture and land use: 1) Areas including one-story buildings and lands covered with grass and scattered trees, highly suitable for research in rural areas; 2) Dense urban areas with high-rise buildings, urban drains, power transmission lines, and low vegetation, suitable for research in urban areas; and 3) Areas without urban texture, covered with grass, trees, canals, and scattered lakes, and suitable for research in non-urban regions. Since the study area was extensive, and the suggested algorithm's findings required repeated field visits, access to the study locations was critical. As a result, the research region was separated into three sections: urban, rural, and without structures, each sector including accessible samples of <2 hectares. Finally, the suggested algorithm assessed 301 hectares of the region, of which 136 hectares were urban areas, 88 hectares belonged to rural areas, and 77 hectares were without buildings.

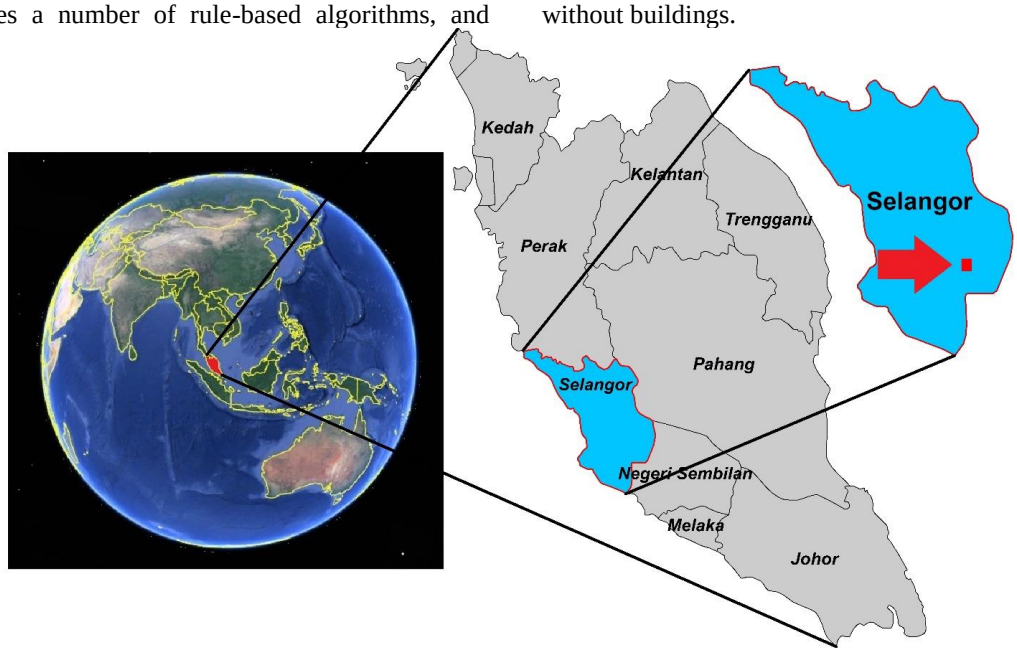

Figure 1: Location of study area

This research used LiDAR data for all processes and RGB images for visual inspection of manual DTM construction and preliminary checking of results. LiDAR point cloud data and orthorectified, used in this research, were acquired in 2015 over Universiti Putra Malaysia and part of the Serdang area by Ground Data Solution Bhd. The raw LiDAR dataset was collected using the Riegel scanner on-board EC-120 Helicopter hovered at an average height above sea level of 600m above the terrain surface. The orthorectified (RGB color image) was captured with the Canon EOS5D Mark III camera with a focal length of 35mm, a horizontal and vertical resolution of 72Dpi, and an exposure time of 1/2500sec. The density of LiDAR data was about 8 points per square meter. This research performed data processing in five steps, all of which were taken automatically in an algorithm written using the Python language.

2.2 Separation of the Last Reflection

Each point in the LiDAR data carries several descriptive data. In the data used in this study, the initial separation is based on the first and last reflections, and the points in the LiDAR data carry a factor known as the 'Classification factor'. Therefore, x, y, and z determine the position of the point in space, and the class factor can determine the first or last reflection. At this stage, the point clouds are converted into a Numpy array, the points with the last reflection are identified, and the other points are removed using the classification factor in the array.

2.3 Calculating the Effective Distance

The designed algorithm compares each point with the surrounding points at a specific distance. More importantly, the effective distance is different for each data, and the above algorithm is designed to automatically calculate the effective distance in each row and between the rows for each different data. The effective distance in each row is larger than the average distance between two points and smaller than twice the average distance between two points, always including at least one point. The effective distance between the rows refers to a distance larger than the average distance between two rows and smaller than twice the average distance between two rows. The average distance between the points in each row is calculated based on Equation 1, and the effective distance in each row is calculated based on Equation 2. However, it is worth noting that this distance is calculated based on the horizontal distance without deviation from the main directions. To operationalize the effective distance, the value that has to be added to the x value of each point is calculated based on Equation 3. D2 is the value whose elimination or addition to the value X of each point will create a range that contains at least two other points except the target point.

$$d1 = \left(\sum_{i=1}^{n-1} \sqrt{\frac{\left(x_{i+1} - x_i\right)^2 + \left(y_{i+1} - y_i\right)^2}{n}} \right)$$

Equation 1

$$d' = d1 + \frac{d1}{2}$$

Equation 2

$$d2 = d' \cdot \cos\alpha$$

Equation 3

$$ax + by + c = 0$$

Equation 4

$$d3 = \frac{1}{m} \sum_{i=1}^{m-1} \frac{|ax + by + c|}{\sqrt{\left(a^2 + b^2\right)}}$$

Equation 5

$$d'' = d3 + \frac{d3}{2}$$

Equation 6

$$d4 = d'' \cdot \sin\beta$$

Equation 7

Where:

x	Value of x axis
y	Value of y axis
i	Number of points
n	Number of points available in LiDAR data
j	Number of rows
m	Number of rows available in LiDAR data
d1	Average distance between the points in row
d2	Effective distance in each row in algorithm
d3	Average distance between rows algorithm
d'	Effective distance between points
d''	Effective distance between rows

The effective distance for each row is also obtained based on the average distance between the rows. Therefore, the line equation for the row is obtained according to Equation 4, and the distance from each point to the line is calculated based on Equation 5, followed by the calculation of the effective distance for that point using Equation 6. The resulting distance actually determines the vertical distance from each point.

To operationalize the results and use them in the designed algorithm, the resulting effective distance has to be converted into a number to be added to and subtracted from the value of y of each point. Therefore, the resulting value is converted to the distance value on the y axis using Equation 7. Based on the calculations above, a range is identified for each point based on the minimum and maximum values calculated on the x and y axes. As a result, at least 4 points are placed around the target point.

2.4 Error Filtering

Errors in LiDAR data are classified into two categories: Type I includes ground points regarded as non-ground points, and type II includes non-ground points accepted as ground points [35]. In urban areas, numerous high-density man-made objects can cause type II errors. Therefore, the filtering stage is substantially important in LiDAR data and can be performed both manually and automatically [4]. The current research has used the nearest neighbor filtering based on the effective distance because this filter can decide according to the features of the data existing in the neighborhood of the target point, and this is fully in line with the selection of a point for the grounds and non-grounds. Furthermore, the research shows that this filter is effective at noises removal [36].

2.4.1 Nearest Neighbor Filter (K-NN)

Here, the effective distance is the range required to analyze the data features. The logic behind this idea is that if the selected point is part of the ground points, most of the points around it fall in the same category, and if a point is a noise, most of its neighboring points do not fall in this category. Therefore, the K-NN filter can remove many noises and the 'roof error' is one of the errors removed with this filter.

2.4.2 Roof error

Laser can enter some objects due to their characteristics and lead to the initial and last reflections. This naturally applies to trees, allowing for the recognition of vegetation. However, in urban areas, this phenomenon occurs in some ceilings through which laser can pass and create what is known as the 'roof error'. These types of structures are not exclusively used in greenhouses with transparent ceilings because urban grounds have various structures, and this error is widely present in a part of the existing structures. Considering the logic used in the neighboring filter based on the effective distance, the K-NN filter can remove the roof error. Pseudo-code as illustrated in Figure 2 is a part of codes written for the K-NN filter automation in the DTM building stage.

2.5 Creating a Modified Network

After filtering the nearest neighbor, many locations lacking data, known as the 'empty spaces', are created. These empty spaces are classified into two categories. The first category includes small spaces created due to the removal of one or two points, and the second category includes large spaces created to remove the structures. In this research, 'large spaces' refer to spaces in which there is no remaining point within the effective window range.

```
Input
Input_array1 (an array that contains all points)
Inpur_array2 (an array that contains points with the last reflection)
Loop
        For I in Input_array2
                (Creating list A of coordinates in the effective window range with point I as the center
                from Input_array1)
                For j in list A
                If (Reflection of point j equals 2):
                        Conter1+=1
                Else
                        Conter2+=1
                If Conter2< Conter1:
                        (Point I is added to list B)
                Conter1= Conter2=0
Output
        Output_array (The coordinates on list B are omitted from Input_array2)
```

Figure 2: Pseudo-code for K-NN filter automation

A new grid of points has been used to fill the empty spaces. The distance between points in the new grid is assumed equal to the minimum distance between the points in LiDAR data and rated based on the elevation value of the points in LiDAR data. Hence, the weighted averages of all the existing points in the LiDAR data, located within the effective window with the center of target point in the new grid of points, are calculated. Therefore, the value of the target point is calculated based on the distance of each LiDAR point, which is in effective window from the target point according to Equation 8. This process is repeated for all the points in the new grid. The value of existing points in the large empty spaces is filled with -999.

$$d = \sqrt{\left(x_{(si)} - x_{(so)}\right)^2 + \left(y_{(si)} - y_{(so)}\right)^2}$$

$$Z_{(so)} = \frac{\sum_{i=1}^{N} \left(\frac{1}{d}\right)^k Z_{(si)}}{\sum_{i=1}^{N} \left(\frac{1}{d}\right)^k}$$

Equation 8

where:

$Z_{(So)}$	Elevation at target point
$Z_{(Si)}$	elevation at point i
i	considered point number at effective distance
n	number of points in effective window
k	impact coefficient of target point distance, which is considered here as 2
s_o	target point
s_i	point i in effective distance

2.6 Interpolation

This stage targets the large empty spaces filled with value -999. First, the boundary of every object is detected because the margins of structures are significantly important in urban planning. This is because a structure is built as a vertical object into the ground, and only the structure boundary is in line with the general earth slope, which is considered in environment planning such as the design of the urban sewage network. Hence, if a structure is removed, the space occupied by the structure has to be filled as a smooth surface in line with the general earth slope. In other words, if the boundary points maintain their effects in the object interpolation, two types of error occur, including stair and surface interpolation errors.

2.6.1 Stair error

Stairs are objects sometimes implemented to connect land to buildings. They are usually seen only in the input section and are not present at all the borders of the building (Figure 3(a)). However, in the design of the urban drains, the general slope of the ground is often followed, which is the same slope of the building border (Figure 3(b)). Hence, the space under the stair is often used to continue the drains (Figure 3(c)). In other words, the stairs connected to the buildings do not act as a barrier against running water. Therefore, when filling the empty spaces, if interpolation is done normally and considering all the existing points in the area, the impact of steps connected to buildings is observed within the buildings limits. In this case, the spaces within the buildings would turn into wavy surfaces instead of being flat (which follow the elevations at the borders of the building). This type of surface could not be a good DTM for the urban area. Here, this type of error, produced due to any object that connects land to a part of the building, is called the "Stair error".

2.6.2 Surface interpolation error

All the existing interpolation algorithms are designed based on data continuity, and the continuous data maintains its effect in the new data up to a certain distance. From there, water flow follows the overall slope of the structure. Therefore, an algorithm has to be used to create a smooth part after interpolation. As a result, the designed algorithm first modifies the boundary of the large empty spaces based on the average height of each side, and interpolation is performed correctly within the range. In this case, the effect of stairs or small structures, which play the role of connectors, is eliminated, and the impact of the height of the sides is not stretched along the structure.

2.7 Create DTM

At this stage, the new point's network, edited in the previous steps based on the coordinate system of LiDAR, is converted to DTM. Therefore, the DTM is created in a fully automatic process from LiDAR data and saved in the TIFF format in the output path.

2.8 Accuracy Assessment

Since the manual DTM has good accuracy [17], the DTM of the area was first manually generated in this section, using the LiDAR point clouds, and both DTMs were compared based on statistical calculations and field visits.

2.8.1 Statistical calculations

A database was created, where each point had two values of DTMs, manual and automatic. Descriptive statistics were used to evaluate the height and slope of the two DTMs. The minimum, maximum, and average height and slope factors of the two DTMs were investigated, and their standard deviation was calculated based on Equation 9. In the next step, the difference between the two layers was examined via the t-test. Finally, the two DTMs were compared to each other based on RMSE because it is an appropriate criterion to examine the amount of error [33] [37] [38] and [39].

$$SD = \sqrt{\frac{1}{N}\sum_{i=1}^{N}\left(x_i - \mu\right)^2}$$

Equation 9

Where:

- N Number of available database points
- I Variable number under review
- x_i i-th variable under review
- μ The mean of the data under review

2.8.2 Field visit

Considering that some differences in the output layers required a field study, a change map for the two DTMs relative to each other was generated, and the coordinates of the changes were extracted from the change map. Next, using the RGB image, the object that caused two different DTMs was determined, and the automatic and manual DTMs were compared in the ArcScene environment in a three-dimensional form. In the next step, using GPS, the mentioned object was found in the study area, and the difference between the two DTMs were subject to field visits.

3. Results

3.1 The First Study Area

The first study area has one-story buildings, narrow roads, and relatively dense tree vegetation that are sometimes very close to the buildings or cover them. Furthermore, the construction of buildings does not follow a particular order, and temporary structures are abundantly scattered everywhere. This region has all the characteristics of rural areas. In Figure 4(a), the building shown with the letter D is considered an object using the algorithm designed in this research, the boundary of the given object is modified based on the designed algorithm, and then interpolation is performed. As a result, the canal on the left side of the building has remained a real canal and does not affect the building environment.

However, in Figure 4(b), which is associated with the manually built DTM, the height of the existing canal directly affects the location of the building due to the lack of the mentioned mechanism. As a result, this canal appears as a series of continuous pits with separating hills, while the building area looks like a pit. Figure 4 clearly shows that the removal of the 'stair error' and the 'surface interpolation error' is necessary to correctly display the building locations and canals. A comparison of the elevation and slope characteristics of the corresponding points in both DTMs shows no significant differences between the elevation factors (Table 1). However, there were evident differences in the slope factor. Next, the value of each DTM was subjected to the independent samples t-test (Table 2), revealing a significant difference between the two DTMs. Although the above test indicated a difference between the two DTMs, the t-test could not show the value of this difference. This issue needs further investigation, considering the correlation of >95% between the two DTMs, the standard deviation value of 0.001m, and the error range of 0.013-0.018m, as it might be impossible to use the difference for specific scales.

Hence, the RMSE value of the DTM layer created automatically was calculated considering the DTM calculated manually. According to the calculations, the RMSE was .05m in the rural areas, indicating that the average difference between automatically and manually calculated DTMs was 5cm. The used maps in the urban and rural planning had the scale of 1:2000[40]; therefore, the error of 5cm is totally acceptable.

3.2 Second Study Area

This area is a prominent example of an urban area. The presence of high-rise buildings, numerous cars, wide streets, and concrete structures such as curbs and short trees compared to the buildings are the characteristics of the second study area, which was examined as an urban area in this study, with the selected samples covering an area of 136 hectares. Field visits showed that many buildings in the second study area have a longitudinal slope and are built as stepped buildings on a slope. However, the manually built DTM is entirely uniform and does not consider the changes made to the earth's surface. Figure 5 shows the location of the investigated samples within the study area while also demonstrating a residential house to better illustrate the longitudinal and lateral slopes and highlighting the difference between the two DTMs.

Figure 3: A view of the design procedure of urban drains with respect to buildings

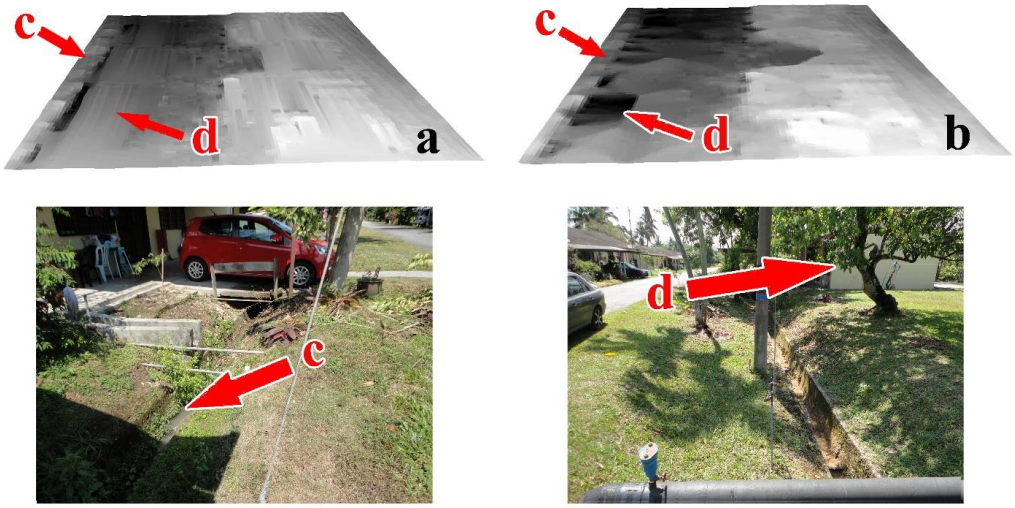

Figure 4: Constructed DTMs. (a) automatically generated DEM (b) Manually generated DEM

Table 1: Slope and elevation specifications of constructed DTMs in first study area

	Height (m)				***Slope (%)***			
	Min	Max	Mean	SD	Min	Max	Mean	SD
Automatic DTM	41.2	42.7	42.2	0.26	0	95.6	5.9	7.5
Manual DTM	41.2	42.7	42.2	0.27	0	88.7	4.7	6.2

Table 2: Comparison of two DTMs based on independent-sample t-test in first study area

	correlation	*t-test for Equality of Means*						
		t	df	Sig	Mean Difference	Std. Error Difference	95% Confidence Interval of the Difference	
							lower	Upper
Equal variances assumed	0.953	13.112	196558	0.000	0.016	0.001	0.013	0.018
Equal variances not assumed		13.112	1.964E5	0.000	0.016	0.001	0.013	0.018

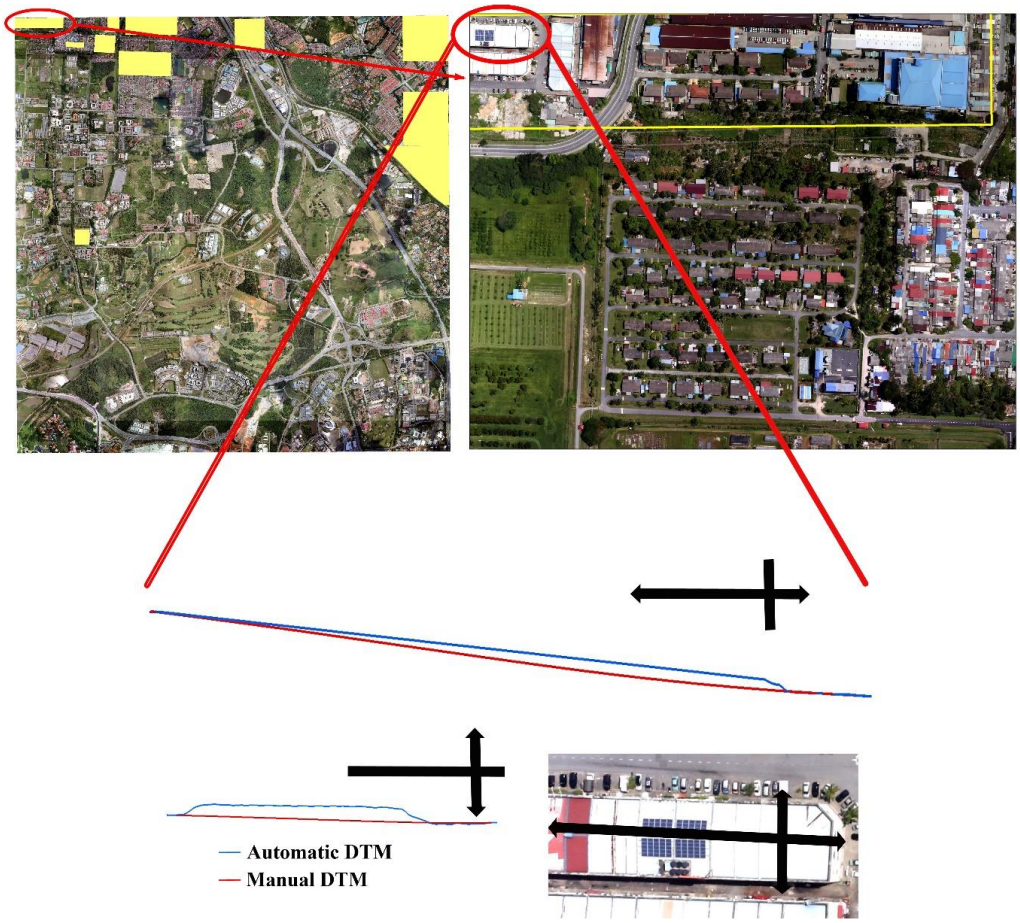

Figure 5: Longitudinal and cross section of manually and automatically constructed DTMs

As clearly seen in Figure 5, the ground at the bottom of the building is slightly hollow in the longitudinal cross-section of the manually built DTM, and it definitely cannot be a suitable model for urban planning. However, the DTM built based on the proposed algorithm fully restores the changed ground shape and shows the increased height at the building downstream. This is manifested in another form in the transverse cross-section of the building.

Here, the comparison of the elevation factors of the two DTMs indicates a slight difference between the study factors. However, an analysis of the existing slope difference revealed a significant difference (Table 3). Seemingly, as the number of urban structures increases, the difference in the average slope increases, and thus the sudden slope changes in urban regions are considerably higher than the rural regions. The statistical test also indicates the difference between two DTMs (Table 4); however, the value of difference is not clear. The correlation of >95% between the two DTMs, standard deviation of 0.007, and an error range of 0.047-.073 confirm the slight difference between the two DTMs. Hence, the RMSE of the DTM layer constructed automatically was also calculated considering the manually-constructed DTM. The calculations show the RMSE value of 0.2m in the urban areas, highlighting that the average difference between the DTMs constructed automatically and manually is 20cm, which is totally acceptable considering the required scale in the urban and rural planning.

3.3 Third Study Area

This area lacks man-made buildings and structures and is covered with grass and scattered trees. Hence, this region is highly suitable to analyze the mechanisms used to build the DTM manually and automatically. The results indicate that as the number of urban structures grows, the difference between the manual and automatic methods is further highlighted. Therefore, if the difference between the two methods used is based on man-made structures, the first hypothesis is that in areas lacking man-made structures, there should be no differences between the two DTMs built.

Table 3: Slope and elevation specifications of constructed DTMs in second study area

	Height (m)				***Slope (%)***			
	Min	Max	Mean	SD	Min	Max	Mean	SD
Automatic DTM	45.8	48.8	47.3	0.79	0	82	6.4	7.9
Manual DTM	45.8	49.2	47.2	0.85	0	66	4.8	5.2

Table 4: Comparison of two DTMs based on independent-sample t-test in second study area

	correlation	*t-test for Equality of Means*						
		t	df	Sig	Mean Difference	Std. Error Difference	95% Confidence Interval of the Difference	
							lower	Upper
Equal variances assumed	0.959	8.706	56472	0.000	0.060	0.007	0.047	0.073
Equal variances not assumed		8.706	5.622E4	0.000	0.060	0.007	0.047	0. 073

Table 5: Slope and elevation specifications of constructed DTMs in third study area

	Height (m)				***Slope (%)***			
	Min	Max	Mean	SD	Min	Max	Mean	SD
Automatic DTM	40.1	41.6	41.0	0.28	0	51.5	9.1	10.1
Manual DTM	40.2	41.6	41.0	0.27	0	53.6	9.1	10.3

Table 6: Comparison of two DTMs based on independent-sample t-test in third study area

	correlation	*t-test for Equality of Means*						
		t	df	Sig	Mean Difference	Std. Error Difference	95% Confidence Interval of the Difference	
							lower	Upper
Equal variances assumed	0.967	-1.790	16534	0.073	-0.008	0.004	-0.016	0.001
Equal variances not assumed		-1.790	16534	0.073	-0.008	0.004	-0.016	0. 001

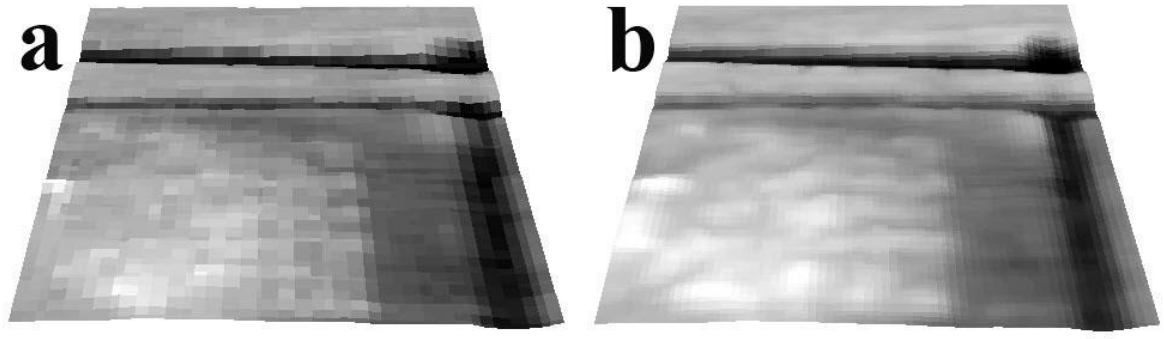

Figure 6: DTMs constructed in third study area. (a) automatically generated DEM (b) Manually generated DEM

Figure 6(a) shows the DTM built using the proposed algorithm, and Figure 6(b) shows the DTM built manually. The results of the field studies confirm the primary hypothesis, according to which there is not a significant difference between the two DTMs. A comparison of the elevation characteristics of the two DTMs also shows many similarities, as confirmed through the comparison of the slope characteristics (Table 5). This is also confirmed by the t-test, and the numbers in the two DTMs linked to one coordinate are not significantly different (Table 6). On the other hand, the RMSE=0.04m exhibits an error equal to 4cm, which is a totally acceptable precision.

4. Discussion

Despite some similarities in the method used here with previous studies, such as using a window to filter noise in neighborhood points [1] [24] and [25], the size of the window does not change based on the features [25] but is automatically calculated based on the data type and the distance of LiDAR points. This issue automatically solves the problem of selecting the window size [25]. Furthermore, the window selected in this research is the basis for comparing each point with other points based on the nearest neighboring filter. Therefore, there is no need to use the slope filter [26] [27] and [38] or classify other grounds [25], and unlike many studies, there is no need for a separate layer or high-accuracy DSM [3] and [30]. This reduces the DTM building cost, accelerating its generation.

The elimination of manual operations is regarded as one of the biggest benefits of this research, because most previous studies have spent a lot of time on expert-based operations [14], increasing the costs and causing non-adherence to the methods designed in executive projects.

In other words, the proposed algorithm removed all the stages that need the specialist intervention and investigation and provided a good accuracy concerning the methods that attempted to generate DTM. For example, Jakovljevic et al., [34] reached the RMSE values in the range 0.05 to 0.25m, although they had investigated their study area before using their proposed method and provided training samples for each area. However, the studied areas in that research included a maximum of 8% urban texture. On the other hand, the RMSE values were 0.04m in area without building and 0.20m in urban area in the current study, using the proposed method, implementing a fully automatic method, and without training samples. Klapste et al., [13] conducted a study in an area without man-made structures, when the trees lacked leaves. They used the common available software for the DTM generation and obtained RMSE values in the range of 0.13 to 0.19m. It is noteworthy that Klapste et al. [13] reviewed the LiDAR points by the specialists and removed the problematic points before using the measured data, whereas the algorithm used in this research was implemented when all trees had leaves, and all the process was conducted automatically. The RMSE values for the areas without buildings and rural areas were 0.04 and 0.05m, respectively.

On the other hand, a review of literature on creating DTM showed that the accuracy of a continuous data-based interpolation method is an advantage over other existing methods [31], and the IDW is an appropriate algorithm for interpolation and construction of DTM [38] and [41]. However, the results of this study show that in areas where severe changes occur in the slope, such as structures and urban and rural canals, using methods based on continuous data for the entire area would not lead to good results. This issue is especially more obvious in the canals close to the buildings. Hence, in the urban and rural areas, one should interpolate the objects apart from lands such as canals and land limits as separate objects, and then fitting should be applied. Thus, according to Figure 4(a), canals would not affect the surrounding objects, and the real image of the ground is preserved. This is also true concerning the stairs. As shown in Figure 3, stairs are small sections to connect buildings and do not affect the overall slope of the area. When the effect of stairs is not removed, some holes would appear in the border of buildings. If the method introduced in this research is implemented, the effect of stairs would be limited to the stairs themselves.

5. Conclusion

It can be concluded from the findings of this research that using the K-NN filter for noise removal in a smart environment is highly effective because it is possible to analyze each point based on the effective distance. Therefore, if the K-NN filter is used based on the effective distance, the noise in the LiDAR data is removed. lthough the statistical test shows the difference between the two DTMs in the urban and rural areas, a correlation of >95% in the generated DTMs and very low standard deviation value show that we cannot confirm the lack of accuracy of DTM just by relying on the difference in the statistical test. The reason is that these tests only reveal the presence of difference but cannot determine whether this difference affects a specific scale or not. Thus, generally, it could be concluded that the DTMs generated by the algorithm used in this research for urban and rural areas and the areas without buildings have appropriate accuracy equal to the accuracy of DTMs generated manually. On the other hand, field surveys confirm that the DTM built using the algorithm proposed in this research is more accurate in areas with higher building densities or buildings near grounds such as canals. The continuous data-based interpolation methods in man-made environments that involve a sudden change in slope are not efficient enough. As shown in Figure 3, the results of manual DTM show the presence of pits in the vicinity of the canals, which are produced due to interpolation and should be examined and edited by specialists.

However, the produced DTM in this research could produce the complete canal shape, interpolating the building in the vicinity of the canal based on the existing algorithm and following the mean slope of the area. In general, it is possible to create a fully automatic structure for the extraction of DTM based on LiDAR data. However, it is worth noting that many filters should be used to create a fully automatic process. Based on these filters, every point has to be compared to the other points surrounding it, necessitating massive computations that can only be performed in a fully smart environment. Therefore, the use of programming languages and artificial intelligence algorithms is the only path to the automation of the mentioned processes. Furthermore, to operationalize the results, the algorithms have to be designed to avoid the need for quantitative and qualitative data except for the initial data. Thus, the Rule-Base Method is highly efficient and does not require training samples.

Finally, it is necessary to use many filters in this research method, based on which any point should be compared to other surrounding points, leading to huge computational tasks. Therefore, access to good hardware will be one of the limitations of this method when producing DTM for a large area. However, based on the field studies in urban and rural areas, the DTM generated by the proposed algorithm is more consistent with the study area than the manually generated DTM. Therefore, it seems as if the manual DTM production process needs further scrutiny due to the specific type of interpolation based on continuous data used in manual DTMs. As a result, it is recommended to carefully investigate the process of manual DTM in separate research employing terrestrial mapping and dual-frequency GPS, as it seems that the commonly used techniques for creating manual DTM in urban areas need significant adjustment.

References

[1] Amini Amirkolaee, H., Enayati, H. and Veisi, M., (2017). Extracting the "Digital Terrain Model" from the Points Cloud by Presenting a Progressive Morphological Method. *Geographic Information Journal*. Vol. 102, 53-68. http:// www.sepehr.org/article_27456.html

[2] Meng, X., Wang, L., Silván-Cárdenas, J. L. and Currit, N., (2008). A Multi-Directional Ground Filtering Algorithm for Airborne LIDAR. *ISPRS J. Photogrammetry and Remote Sensing*. Vol. 64(1), 117–124.

[3] Perko, R., Raggam, H., Gutjahr, K. H. and Schardt, M., (2015). Advanced DTM Generation from Very High Resolution Satellite Stereo Images. *ISPRS Ann. Photogrammetry and Remote Sensing. Spatial Inf. Sci.*, Vol. II-3/W4, 165–172. https://doi.org/10.5194/isprsannals-II-3-W4-165-2015

[4] Seif, A. and Mahmoodi, T., (2013). LiDAR Sensor and its Applications. *Journal of Geographical Information*. Vol. 23(89), 72-80, http://www.sepehr.org/article_13059.html

[5] Geiß, C., Aravena, P., Marconcini, M., Sengara, W. and Edwards, M., (2015). Estimation of Seismic Building Structural Types Using Multi-Sensor Remote Sensing and Machine Learning Techniques. *ISPRS J. Photogramm Remote Sens.*, Vol. 104, 175-188. https://doi.org/10.1016/j.isprsjprs.2014.07.016

[6] Askne, J. I. H., Soja, M. J. and Ulander, L. M. H., (2017). Biomass Estimation in a Boreal Forest from TanDEM-X Data, Lidar DTM, and the Interferometric Water Cloud Model. *Remote Sensing of Environment*. Vol. 196, 265–278, https://doi.org/10.1016/j.rse.2017.05.010

[7] Martha, T. R., Kerle, N., Jetten, V., Van Westen, C. J. and Vinod Kumar, K. (2010). Landslide Volumetric Analysis Using Cartosat-1-Derived DEMs. *IEEE Geosci. Remote Sens. Lett.*, Vol. 7(3), 582–586.

[8] Nahhas, F., Shafri , H. Z. M., Sameen, M., Pradhan, B. and Mansor, Sh., (2018). Deep Learning Approach for Building Detection Using, LiDAR Orthophoto Fusion. *Journal of Sensors*. 1-12. https://doi.org/10.1155/2018/7212 307

[9] Razak, K. A., Straatsma, M. W., Van Westen, C. J., Malet, J. P. and De Jong, S. M., (2011). Airborne Laser Scanning of Forested Landslides Characterization: Terrain Model Quality and Visualization. *Geomorphology*. Vol. 126(1–2), 186–200. https://doi.org/10.1016/j.geomorph.2010.11.003

[10] Bujan, S. Sellers, C. A. Cordero, M. and Miranda, D., (2020). DecHPoints: A New Tool for Improving LiDAR Data Filtering in Urban Areas. *PFG – Journal of Photogrammetry, Remote Sensing and Geoinformation Science*, Vol. 88, 239–255. https://doi.org/10.1007/s41064-019-00088-7

[11] Jin, S., Su, Y., Zhao, X., Hu, T. and Guo, Q., (2020). A Point-Based Fully Convolutional Neural Network for Airborne LiDAR Ground Point Filtering in Forested Environments. *IEEE Journal of Selected Topics in Applied Earth Observations and Remote Sensing*. Vol. 13, 3958-3974, https://doi.org/10.1109/JSTARS.2020.3008477

[12] Cosenza, D. N., Gomes Pereira, L., Guerra-Hernández, J. Pascual, A., Soares, P. and Tomé, M., (2020). Impact of Calibrating Filtering Algorithms on the Quality of LiDAR-Derived DTM and on Forest Attribute Estimation through Area-Based Approach. *Remote Sens.*, Vol. 12(6). https://doi.org/10.3390/rs12 060918

[13] Klapste, P., Fogl, M., Bartak, V., Gdulova, K., Urban, R. and Moudry, V., (2020). Sensitivity Analysis of Parameters and Contrasting Performance of Ground Filtering Algorithms with UAV Photogrammetry-Based and LiDAR Point Clouds. *International Journal of Digital Earth*. Vol.13(12), 1672-1694. https://doi.org/10.1080/17538947.2020.1791267

[14] Mason, D., Horritt, M., Hunter, N. and Bates, P., (2007). Use of Fused Airborne Scanning Laser Altimetry and Digital Map Data for Urban Flood Modelling. *Hydrological Processes*. Vol. 21(11), 1436–1447. https://doi.org/10.1002/hyp. 6343

[15] Flood, M., (2001). *LiDAR Activities and Research Priorities in the Commercial Sector. International Archives of the Photogrammetry, Remote Sensing and Spatial Information Sciences*. https://www.isprs.org/proceedings/XXXIV/3-W4/pdf/Flood.pdf

[16] Fowler, A., (2000). The Lowdown on LiDAR. *Earth Observation Magazine*. http://www.lidar.com.br/arquivos/lidar.pdf

[17] Sreedhar, M., Muralikrishnan, S. and Dadhwal, V. K., (2015). Automatic Conversion of DSM to DTM by Classification Techniques Using Multi-date Stereo Data from Cartosat-1. *Journal of the Indian Society of Remote Sensing*. Vol. 43, 513–520, https://link.springer.com/article/10.1007/s12524-014-0410-8

[18] Liu, X., (2008). Airborne LiDAR for DEM Generation: Some Critical Issues. *Progress in Physical Geography*. Vol. 32(1), 31-49, https://doi.org/10.1177%2F0309133308089496

[19] Sithole, G. and Vosselman, G., (2004). Experimental Comparison of Filter Algorithms for Bare-Earth Extraction from Airborne Laser Scanning Point Clouds. *ISPRS Journal of Photogrammetry & Remote Sensing*. Vol. 59(1–2), 85– 101. https://doi.org/10.1016/j.isprsjprs.2004.05.004

[20] Meng, X., Currit, N. and Zhao, K., (2010). Ground Filtering Algorithms for Airborne LiDAR Data: A Review of Critical Issues. *Remote Sensing*. Vol. 2(3), 833-860, https://doi.org/10.3390/rs2030833.

[21] Farshad, A. and Farzaneh, A., (2018). *Application of Remote Sensing Data and GIS in Sustainable Agricultural Development, Conservation of Natural Resources and Environment of Iran with Special Attention to the Use of Analog/Digital Aerial Photographs, Satellite-Hyperspectral Images, Satellite Positioning, Radar and LiDAR*. Iran Watershed Management Association Research Project Report (book), Second edition. 60-79

[22] Abdullah, A. F., Rahman, A. A. and Vojinovic, Z., (2009). Lidar Filtering Algorithms for Urban Flood Application: Review on Current Algorithms and Filters Test. In: Bretar F, Pierrot-Deseilligny M, Vosselman G (Eds) Laser scanning, IAPRS. Vol. xxxviii, Part 3/W8 – Paris, France, September 1-2. 3-36.

[23] Atirah Muhadi, N., Fikri Abdullah, A., Khairunniza Bejo, S., Razif Mahadi, M. and Mijic, A., (2020). The Use of LiDAR-Derived DEM in Flood Applications. *A Review Remote SensingJournal*. Vol.12(14). https://doi.org/10.3390/rs12142308

[24] Kilian, J., Haala, N. and Englich, M., (1996). Capture and Evaluation of Airborne Laser Scanner Data. *International Archives of Photogrammetry and Remote Sensing*. Vol. 31, 383-388.

[25] Zhang, K., Chen, Sh., Shyu, M., Yan, J. and Zhang, Ch., (2003). A Progressive Morphological Filter for Removing Nonground Measurements from airborne LiDAR Data. *IEEE Transactions on Geoscience and Remote Sensing*. Vol. 41(4). 872 –882. https://doi.org/10.1109/TGRS.2003.810682

[26] Vosselman, G., (2000). Slope Based Filtering of Laser Altimetry Data. *International Archives of Photogrammetry and Remote Sensing*. Vol. 33, 935-942.

[27] Sithole, G., (2001). Filtering of Laser Altimetry Data Using a Slope Adaptive Filter. *International Archives of Photogrammetry and Remote Sensing*. Vol. XXXIV-3/W4, 22-24. https://citeseerx.ist.psu.edu/viewdoc/download?doi=10.1.1.151.62&rep=rep1&type=pdf

[28] Sohn, G. and Dowman, I., (2002). Terrain Surface Reconstruction by the Use of Tetrahedron Model with the MDL Criterion. *International Archives of Photogrammetry Remote Sensing and Spatial Information Sciences*. Vol. 34, 336-344.

[29] Baligh Jahromi, A., Zoej, M. J. V., Mohammadzadeh, A. and Sadeghian, S., (2011). A Novel Filtering Algorithm for Bare-Earth Extraction from Airborne Laser Scanning Data Using an Artificial Neural Network. *IEEE Journal of Selected Topics in Applied Earth Observations and Remote Sensing*. Vol. 4(4), 836–843, https://doi.org/10.1109/JSTARS.2011.2132793

[30] Zhang, Y., Zhang, Y., Zhang, Y. and Li, X., (2016). Automatic Extraction of DTM from Low Resolution DSM by Twosteps Semi-Global Filtering. *ISPRS Annals of the Photogrammetry, Remote Sensing and Spatial Information Sciences*. Vol. III-3, 249-255. https://doi.org/10.5194/isprs-annals-III-3-249-2016

[31] Wojciech, M., (2018). Kriging Method Optimization for the Process of DTM Creation Based on Huge Data Sets Obtained from MBESs. *Geosciences.* Vol. 8(12). https://doi. org/10.3390/geosciences8120433

[32]Chen, Z., Devereux, B., Gao, B. and Amable, G., (2012). Upward-Fusion Urban DTM Generating Method Using Airborne Lidar Data. *ISPRS Journal of Photogrammetry and Remote Sensing*, Vol. 72, 121-130. https://doi.org/10.1016/j.isprsjprs.2012.07.001

[33] Vernimmen, R., Hooijer, A. and Pronk, M., (2020). New ICESat-2 Satellite LiDAR Data Allow First Global Lowland DTM Suitable for Accurate Coastal Flood Risk Assessment. *Remote Sens*., Vol. 12. https://doi.org/10.3390/rs12172827

[34] Jakovljevic, G., Govedarica, M., Alvarez-Taboada, F. and Pajic, V., (2019). Accuracy Assessment of Deep Learning Based Classification of LiDAR and UAV Points Clouds for DTM Creation and Flood Risk Mapping. Geosciences, Vol. 9(7). https://doi.org/10.3390/geosciences9070323

[35] Pfeifer, C. B. N. and Stadler, P., (2001). *Derivation of Digital Terrain Models in the Scop++Environment.* OEEPE Workshop on Airborne Laser scanning and Interferometric SAR for Digital Elevation Models, Stockholm. https://mrs.geo.tuwien.ac.at/media/filer_public/c8/22/c8226740-9630-4a82-9147-15ba94e7df50/np_stockholm.pdf.

[36] Shirowzhana, S., Limb, S., Trinderb, J., Lic, H. and Sepasgozara, S. M. E., (2020). Data Mining for Recognition of Spatial Distribution Patterns of Building Heights Using Airborne Lidar Data. *Advanced Engineering Informatics*. Vol. 43. https://doi.org/10.1016/j.aei.2020.101033

[37] Giannettia, F., Pulettib, N., Pulitic, S., Travaglinia, D. and Chiricia, Gh., (2020). Assessment of UAV Photogrammetric DTM-independent Variables for Modelling and Mapping Forest Structural Indices in Mixed Temperate Forests. *Ecological Indicators*. Vol. 117. https://doi.org/10.1016/j.ecolind.2020.10 6513

[38] Bigdeli, B., Gomroki, M. and Pahlavani, P., (2018). Generation of Digital Terrain Model for Forest Areas Using a New Particle Swarm Optimization on LiDAR Data. Survey Review. Vol. 52(371), 115-125. https://doi.org/10.1080/00396265.2018.1530331

[39] Cateanu, M. and Ciubotaru, A., (2020). Accuracy of Ground Surface Interpolation from Airborne Laser Scanning (ALS) Data in Dense Forest Cover. *ISPRS International Journal of Geo-Information*, Vol. 9(4). https://doi.org/10.3390/ijgi9040224

[40] Miriam Villar-Cano, M., Jesús Jiménez-Martínez, M. and Marqués-Mateu, A., (2019). A Practical Procedure to Integrate the First 1:500 Urban Map of Valencia into a Tile-Based Geospatial Information System. *ISPRS Int. J. Geo-Inf*. Vol. 8(9). https://doi.org/10.3390/ijgi8090378

[41] Agüera-Vega, F. Agüera-Puntas, M. Martínez-Carricondo, P. Mancini, F. and Carvajal, F., (2020). Effects of Point Cloud Density, Interpolation Method and Grid Size on Derived Digital Terrain Model Accuracy at Micro Topography Level. *International Journal of Remote Sensing*, Vol. 41(21), 82818299, https://doi.org/10.1080/01431161.2020.1771788